Nanochem Res 9(2): 113-137, Spring 2024

RESEARCH PAPER

Enhancing Internal Temperature Control in Student Residential Colleges: Investigating the Potential of Retrofitting Rainwater Collection Tanks

Yue Zhang, Ati Rosemary Binti Mohd Ariffin*

Department of Architecture, Faculty of Built Environment, Universiti Malaya, 50603, Kuala Lumpur, Malaysia

ARTICLE INFO

Article History:
Received 15 January 2024
Accepted 20 March 2024
Published 15 April 2024

Keywords:
Retrofitting rainwater collection tanks
Internal temperature control
Passive cooling strategies
Thermal efficiency
Energy

ABSTRACT

This study investigated the potential of retrofitting rainwater collection tanks (RWH) into the facades of student residential colleges to improve internal temperature control. Carbon nanomaterials, including carbon nanotubes (CNTs) and graphene, were incorporated into the RWH facades to enhance thermal conductivity and mechanical strength. The aim was to address urbanization and climate change challenges through passive cooling strategies. The study analyzed ambient temperature, relative humidity, and wall surface temperature based on heat transfer principles. Statistical attributes, such as maximum, minimum, and average values, as well as daily fluctuations were examined. Heat transmission from external to internal walls was also quantified. Materials analysis in this study involved the utilization of X-ray diffraction (XRD) for phase analysis, scanning electron microscopy (SEM) for investigating the morphology of CNTs, and transmission electron microscopy (TEM) for further characterization. The results demonstrated the cooling effectiveness and thermal efficiency of the proposed RWH technology. The west-facing walls with RWH facades showed a remarkable cooling effect of up to 14.41°C compared to non-RWH counterparts. Similarly, east-facing walls equipped with RWH facades exhibited a maximum temperature reduction of 3.41°C. Carbon nanomaterials enhanced the structural integrity of the RWH facades, ensuring long-lasting reliability under challenging conditions. This study highlighted the effectiveness of RWH facades as passive cooling strategies for student residential colleges. The utilization of carbon nanomaterials further enhanced their thermal and mechanical properties. The results indicated valuable insights for improving internal temperature control and addressing climate change challenges in urban environments.

How to cite this article
Zhang Y., Ariffin A.R.M. Enhancing Internal Temperature Control in Student Residential Colleges: Investigating the Potential of Retrofitting Rainwater Collection Tanks. Nanochem Res, 2024; 9(2):113-137. DOI: 10.22036/ncr.2024.02.004

INTRODUCTION

Materials that prevent the loss of energy in walls play a crucial role in improving thermal efficiency and reducing energy consumption in buildings. One such material is carbon, which offers desirable properties for energy conservation and is increasingly being used in building materials. Carbon-based materials possess excellent thermal conductivity, allowing for efficient heat transfer. This characteristic enables them to effectively regulate temperature imbalances and reduce energy loss through walls. Carbon-based materials, such as carbon fiber or carbon nanotubes, exhibit high thermal conductivity, making them ideal for applications where heat transfer is desired. Furthermore, carbon-based materials are known for their lightweight nature [1-4].

* Corresponding Author Email: *aa_alambina@um.edu.m*

This property offers advantages in construction, as lighter materials can facilitate easier handling and installation, reducing labor and construction costs. Additionally, the lightweight nature of carbon-based materials allows for reduced structural load on buildings, making them suitable for various architectural designs. Rapid urban expansion and development in many tropical cities have led to environmental challenges, including urban heat islands, climate change, and global warming [1]. Ensuring a comfortable indoor environment has become a significant consumer of energy in residential buildings [2]. Previous studies in Malaysia have shown that air conditioner (AC) usage accounts for 57% of total energy consumption [3]. Therefore, efforts have been made to reduce energy consumption through passive cooling design and renewable resources. In tropical regions, improving cooling system efficiency is crucial for achieving sustainable development, implementing the "3R" guideline (reduce, reuse, recycle), and fostering low-carbon economies in the built environment industry to mitigate the impact of extreme weather events such as global warming and urban heat islands, while promoting ecological balance [4]. In the late 1960s, Fanger introduced the Predicted Mean Vote (PMV) model, which has since been widely used globally to assess thermal comfort [5]. Fanger's model was originally designed for air-conditioned buildings in moderately hot climates with stable ambient temperatures, based on research conducted among students [5]. The built environment industry offers various rainwater tank designs for dwellings and related facilities, enabling water conservation and backup during dry spells. However, there has been limited research on integrating rainwater harvesting (RWH) tanks across entire facades as barriers to reduce heat gain. In addition, studies on facade designs for optimal thermal comfort in tropical climates, specifically in residential colleges, are still in their early stages. Previous research has mostly been theoretical and insufficient in understanding the installation, functionality, and efficiency optimization of rainwater tanks for rainwater collection and heat conduction prevention [6-10]. Therefore, it is crucial to conduct comprehensive research to understand the cooling performance of RWH facades on common wall materials. Imessad et al. (2014) investigated the impact of passive cooling techniques on the energy demand of residential buildings in a Mediterranean climate [9]. Mohammed et al. (2006) conducted a study on the potential uses of RWH in urban areas [10]. Ayog et al. (2015) conducted a feasibility study of RWH in the residential colleges of Universiti Malaysia Sabah to support the Eco-Campus Initiative [11]. Shaari et al. (2008) discussed the potential of RWH for improving the quality of living [12]. Rao and Mustapa (2021) conducted a comprehensive review of climate economic models in Malaysia [13]. Instead of relying solely on traditional air conditioning, the installation of RWH tanks on residential college facades offers the potential for passive cooling throughout the building's lifespan. To address current issues related to cooling load, rainwater resource utilization, environmental awareness, and climate change [11-12], a rainwater tank was installed on the front of the residential college. However, further research is needed to maximize the utilization of rainwater resources and regulate indoor ambient temperature effectively. This article aimed to address the existing research gap and explore a novel approach by investigating the integration of RWH tanks on entire facades of residential colleges for enhanced thermal comfort in tropical climates. The objective was to study the performance and effectiveness of rainwater tank facades as barriers to reduce heat gain, optimize rainwater collection, and prevent heat conduction. By conducting comprehensive research, the article sought to contribute to the knowledge base regarding the cooling effect of RWH facades on common wall materials, and provide insights into sustainable building practices that utilize rainwater resources while regulating indoor ambient temperature. The novelty lies in the holistic examination of the installation, functionality, and efficiency optimization of rainwater tanks as passive cooling mechanisms, offering a potential alternative to traditional air conditioning and promoting environmental awareness and climate resilience in the built environment industry.

MATERIALS AND METHODS

Experimental study

Case Study & Outline of Fieldwork

The case study for this research was conducted in Kuala Lumpur, Malaysia (3°08'N, 101°42'E), which exhibits typical weather characteristics of high temperature, humidity, intense solar radiation, and abundant rainfall [13]. The case study conducted in Kuala Lumpur, Malaysia (3°08'N, 101°42'E) represents a typical tropical climate characterized

by high temperature, humidity, intense solar radiation, and abundant rainfall [13]. Specifically, the research focused on a residential college zone in Universiti Malaya, chosen due to its alignment with the selection criteria: (1) the equatorial location of Kuala Lumpur, which experiences intense solar radiation, (2) the requirement for residential college facades to face east or west to measure solar radiation and solar gain, and (3) the need for limited external shadows and sufficient solar radiation. The challenges posed by post-pandemic restrictions and residential college regulations were carefully considered during the case study selection process. The research aims to bridge the identified research gaps and limitations by conducting a thorough literature review and comparing the findings with prior studies on RWH passive cooling [14-17]. The experiment also required spaces facing east and west facades with no occupation and non-air-conditioned spaces with functional windows as shown in Fig. 1. Two identical dorm rooms with the same configuration and layout constituting the experimental setup was selected and used in this study. Each room had internal dimensions of 4.2 m×4.0 m×3.0 m (occupies the area of 16.8 m^2) to perform data collection. Both rooms were unoccupied throughout the experimental process. Essentially, the orientation of the block related to solar radiation, environmental factors, and internal space were regarded when selecting the measured dormitory rooms. Both rooms had windows facing north and south and identical orientations. The design of the windows adopted the louvers, and windows' location was also North-South orientation. There were two louvers in every dormitory room, and the size of the window was 170mm*102mm, and the total area of two windows in every dormitory room was 3.47m^2. Site observations on each dormitory room used for data collection were also conducted to assess real-world circumstances and guarantee the experiment's success, as the floor plan and the exterior view. Retrofitting rainwater collection tanks (RWH) involves the installation of these tanks into existing structures to harness and utilize rainwater resources. This innovative approach offers numerous benefits, such as reducing reliance on traditional water sources, mitigating stormwater runoff, and promoting sustainable water management. Integrating RWH systems into buildings, enables the capture and storage of rainwater for various uses, including irrigation, toilet flushing, and laundry. RWH tanks not only contributes to water conservation but also supports environmental sustainability and resilience in the face of water scarcity and climate change.

Fig. 1 displays a SEM image that highlights the morphology and surface characteristics of the CNTs investigated in this study. The SEM technique enables high-resolution imaging and detailed examination of the sample. The image reveals elongated CNT structures with a tubular shape, exhibiting a smooth and uniform surface indicative of a high level of structural integrity. This SEM image provides crucial insights into the size of 60-120 nm, 20-30 nm as a diameter, and overall quality of the CNTs, which plays a vital role in comprehending their properties and potential

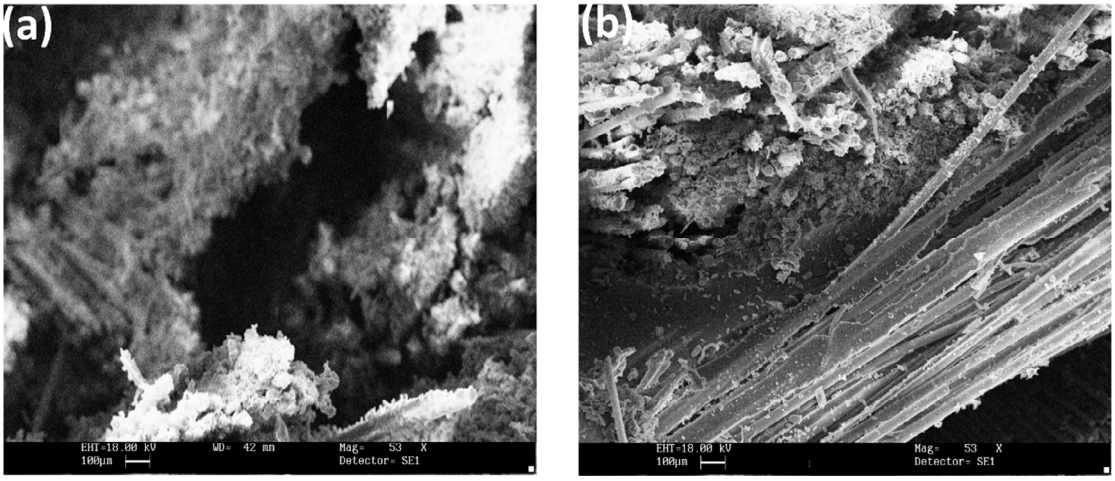

Fig. 1. SEM image of CNTs used as a case study in this study

applications. Carbon nanomaterials, such as CNTs and graphene, have garnered significant attention in various fields due to their exceptional properties. CNTs are cylindrical structures composed of carbon atoms arranged in a unique lattice pattern, providing them with remarkable mechanical strength, high thermal conductivity, and excellent electrical properties. These properties make CNTs promising candidates for reinforcing materials and enhancing the performance of composite systems. Graphene, on the other hand, is a two-dimensional carbon allotrope consisting of a single layer of carbon atoms arranged in a hexagonal lattice. Graphene exhibits extraordinary mechanical strength, superior thermal conductivity, and remarkable electrical properties, making it a desirable material for a wide range of applications. To visualize the morphology and structure of the carbon nanomaterials, SEM was employed. The SEM image shown in Fig. 1 reveals the characteristic morphology of carbon nanotubes. The image exhibits the tubular structure of the CNTs, demonstrating their cylindrical shape and nanoscale dimensions. The SEM analysis allows for the examination of the surface features, including the alignment, dispersion, and agglomeration of CNTs, which critically influence their performance when incorporated into materials. The SEM image provides a visual representation of the unique morphology of carbon nanotubes, illustrating their potential for enhancing the properties of the rainwater collection tank facades.

Quantitative Research Approach

Fig. 2 illustrates the utilization of a quantitative research methodology [18] in conjunction with a deductive theory and experimental approach to validate theories or hypotheses regarding heat transmission through existing and proposed walls. By employing this research methodology, the study aimed to achieve its research objectives [19-21] and enhance the reliability and objectivity of the gathered data. This methodology is crucial in confirming the indoor cooling effect of the RWH tank integrated into the existing wall, providing valuable insights into the effectiveness of the proposed approach.

Parameter & Measuring Equipment

In order to effectively support the research objectives concerning the improvement of indoor thermal comfort and the evaluation of passive cooling performance, this study established specific parameters. These parameters encompassed the measurement of internal and external surface temperatures for the east, west, and south walls, as well as the monitoring of indoor ambient temperature, relative humidity, outdoor ambient temperature, and relative humidity. To acquire surface temperature data, thermocouples (Type T, copper-constantan) with an accuracy of 1.0°C or 0.75 percent above 0°C were utilized. To minimize deviations, four distinct sensor points were employed on each surface. Moreover, HOBO data loggers (U12-012) were applied to measure indoor and outdoor ambient temperature, as well as relative humidity, ensuring comprehensive data collection for the study [22-23].

Experimental Procedures

The data collection process was conducted from 21st March, 2022 to 4th April, 2022, spanning two consecutive weeks, which is recognized as one of the hottest months in Malaysia according

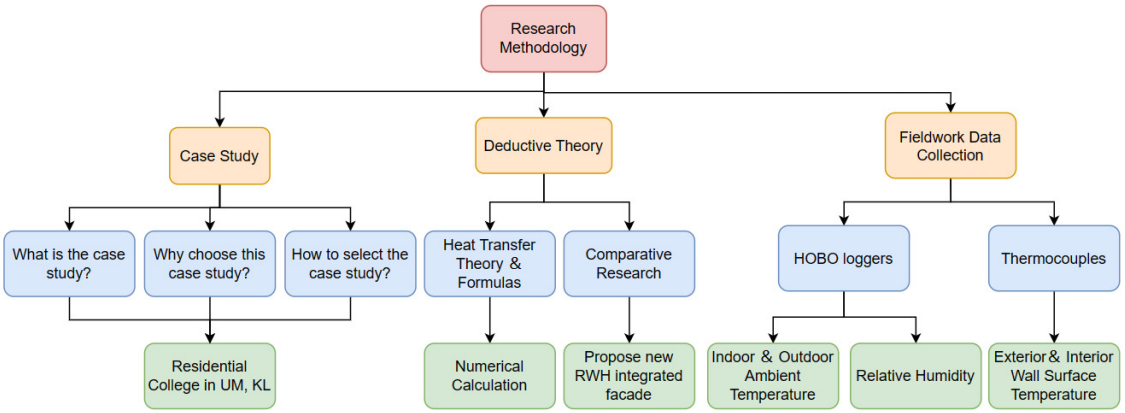

Fig. 2. Research activities framework

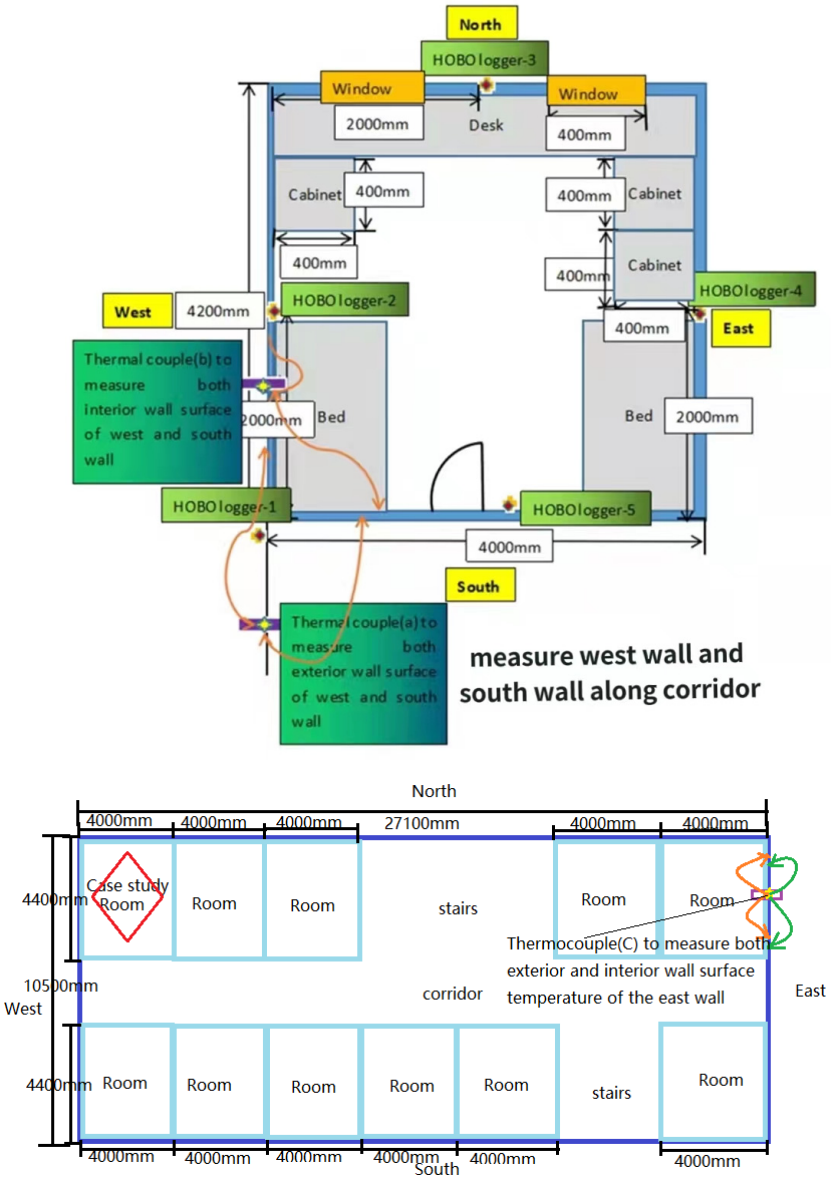

Fig. 3. The architectural plan layout of the installation of HOBO loggers and thermocouples (a) in the dormitory room; (b) on the east wall surface of the block; (c)

to meteorological data. During the experiments, measurements were taken in two different dormitory rooms: one on the fourth level and the other on the first level. The fourth-level room was chosen to capture higher solar radiation due to its elevated position. The first-level room served as a point of comparison. This selection allowed for a comprehensive assessment of the dormitory block, considering the varying levels of solar radiation intensity. Additionally, a separate validation experiment was conducted from 8th July to 15th July, 2022 to further verify the data and experimental results [23-24]. Both dormitory rooms were located on the same floor and had the same configuration and layout to facilitate accurate comparisons. The empirical work aimed to differentiate the two rooms under different experimental conditions and confirm the potential of the RWH tank in reducing indoor temperature and enabling passive cooling [25]. The instruments used for measurement were attached to a stand positioned 1.5 meters above the ground, representing the overall level within the room. This height, closer to the height of a human body, was deemed suitable for assessing occupants'

indoor thermal comfort. To mitigate the impact of rain and flushing, the two HOBO loggers used to measure external temperature in the corridor were mounted at a height of 2 meters. The installation height accounted for the presence of a canopy in the hallway corridor, preventing the instruments from getting wet. The equipment installation height and location remained consistent throughout the two-series experiment to control variables and minimize potential errors. All instruments were calibrated prior to the onsite measurement to ensure accurate data collection. The X-ray Diffraction (XRD) pattern analysis of materials used in these projects provided valuable insights into their structural properties and crystalline nature. By examining the XRD patterns, researchers can gain a deeper understanding of the composition, crystal phase, and crystallographic orientation of the materials, which can be crucial for optimizing their performance in various applications.

Numerical modeling

The experimental process, including the installation of HOBO loggers and thermocouples, as well as the architectural plan for device insulation, is depicted in the schematic diagram presented in Fig. 4. The specific locations for installing the equipment are illustrated in Figs. 4-6.

Fig. 3 illustrates the architectural plan layout for the installation of HOBO loggers and thermocouples in the dormitory room and on the east wall surface of the block. The installation locations were carefully chosen to capture relevant temperature data and monitor the thermal behavior of the studied area. In Fig. 3(a), the placement of HOBO loggers and thermocouples inside the dormitory room allows for the measurement of the internal temperature, providing insights into the indoor thermal conditions experienced by the occupants. This data is crucial for assessing the effectiveness of the retrofitting strategies and their impact on improving internal temperature control. Additionally, Fig. 3(b) depicts the positioning of HOBO loggers and thermocouples on the east wall surface of the block. This placement enables the monitoring of the external surface temperature, which is influenced by factors such as solar radiation and ambient conditions. By tracking the temperature variations on the east wall surface, the study can evaluate the effectiveness of the retrofitting techniques in reducing heat gain and enhancing thermal comfort within the dormitory. We labeled the five HOBO loggers and three thermocouples and put them in different positions to measure indoor and outdoor ambient temperature, relative humidity, and the wall surface temperature of west, east, and south wall in different directions.

Fig. 4 presents images showcasing the installation of HOBO loggers and thermocouples in different areas. In Fig. 4(a), the installation is depicted on the hallway, highlighting the strategic placement of HOBO loggers and thermocouples to capture temperature data in this specific location. This setup allows for the monitoring of the hallway's internal temperature, providing valuable information about the thermal

(a) (b)

Fig. 4. Images of (a) The installation of the HOBO loggers and thermocouples on the hallway; (b)The installation of thermocouple on the corridor to measure the external surface temperature of the west and south walls.

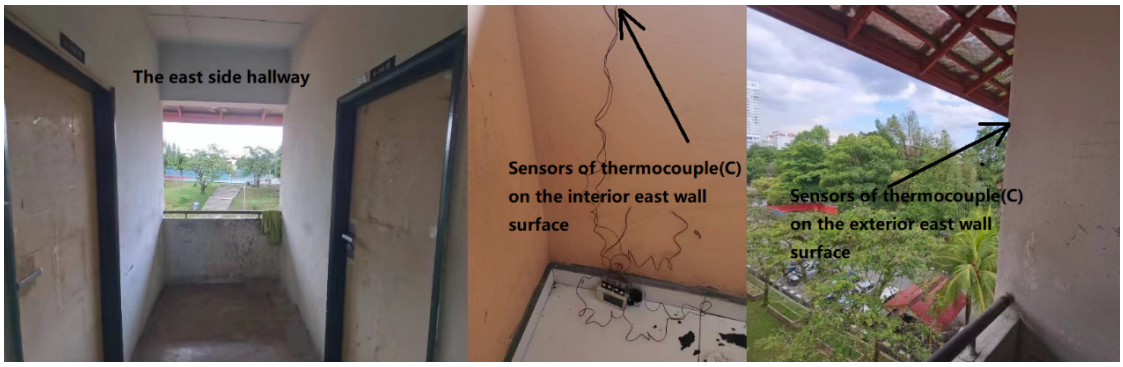

Fig. 5. Images of the installation of thermocouple(C) on the hallway to measure the exterior and interior east wall surface temperature

Fig. 6. Images of (a) installation of equipment on the north wall; (b) installation of equipment on the west wall; (c) installation of equipment on the east wall; (d) installation of equipment on the south wall

conditions experienced in this shared space. These measurements contribute to the overall assessment of the effectiveness of the retrofitting strategies in controlling the temperature within the residential college.

Fig. 5 displays images illustrating the installation of a thermocouple (C) on the hallway, specifically aimed at measuring the temperature of the exterior and interior surfaces of the east wall. This installation is strategically positioned to gather data on both the external and internal temperatures of the east wall, providing valuable insights into its thermal behavior.

Fig. 6 presents a series of images showcasing the installation of equipment in various locations. The images depict the placement of equipment on the north, west, east, and south walls, highlighting the strategic positioning of monitoring devices to capture temperature data and monitor the thermal behavior of each wall. Additionally, an authentic scene of the installation of HOBO loggers and thermocouples in the dormitory room is shown, demonstrating the comprehensive temperature monitoring in different directions within the space. These installations provide valuable insights into the thermal characteristics of the walls and areas within the residential college, enabling a thorough assessment of the retrofitting strategies' effectiveness in improving temperature control and overall thermal performance. Two series of experiments were conducted for the models, both keeping the windows closed in the former three days and keeping the windows open in the latter four days, to evaluate the ability to prevent heat from entering indoor room and improve indoor thermal comfort in residential college dwellings

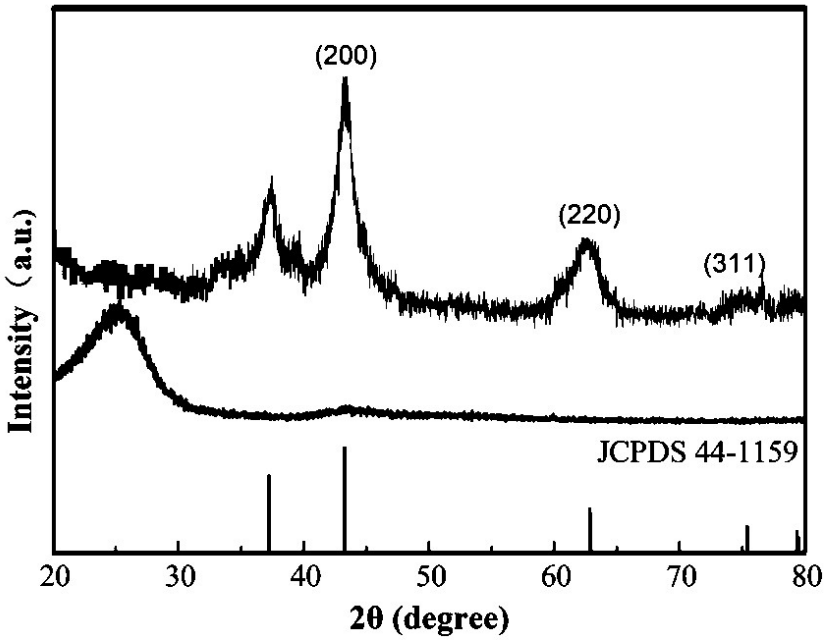

Fig. 7. XRD pattern of Nano materials used in the walls of houses and bodies have favorable mechanical and thermal properties.

[26-27].

Fig. 7 illustrates the X-ray Diffraction (XRD) pattern of the nano materials employed in the walls of houses and bodies, indicating their desirable mechanical and thermal properties. The XRD pattern analysis is a crucial tool in characterizing the crystalline structure of these materials, allowing for the identification of specific crystal phases and the evaluation of crystallographic orientation. By leveraging this information, researchers and engineers gain valuable insights that aid in the optimization of material properties for enhanced energy efficiency, durability, and final performance in sustainable construction. The XRD analysis enables a detailed understanding of the materials' structural characteristics, facilitating the tailoring of their properties to meet the specific requirements of energy-efficient building projects. This knowledge empowers the development of innovative solutions that contribute to the reduction of energy consumption and the promotion of sustainable practices in the construction industry. The XRD analysis helps identify the crystal phases present in the carbon material, which can include graphite, diamond, or amorphous carbon. The presence of specific crystal phases influences the material's mechanical properties, thermal conductivity, and electrical behavior. A highly oriented graphite structures in carbon materials contribute to their excellent thermal conductivity and mechanical strength.

RESULTS & DISCUSSION

Fluctuation Analysis & Maximum, Average value analysis

Outdoor & Indoor Ambient Temperature

The use of carbon-based materials in building materials extends beyond energy conservation. They offer durability, resistance to corrosion and fire, and can be applied in various forms, including sheets, coatings, and composites. This versatility allows for their integration into existing building systems without significant modifications, making them a viable option for energy-efficient retrofitting projects. The XRD pattern obtained from the analysis typically displays characteristic diffraction peaks, which correspond to the interatomic spacing within the crystal lattice. By comparing these diffraction peaks with established databases, researchers can identify the crystal phases present in the material. This information is crucial for understanding the material's structural stability, as different crystal phases may exhibit varying mechanical, thermal, and electrical properties. As shown in Fig. 8, the outdoor ambient temperature in 24 hours arrived at the highest point on 27th

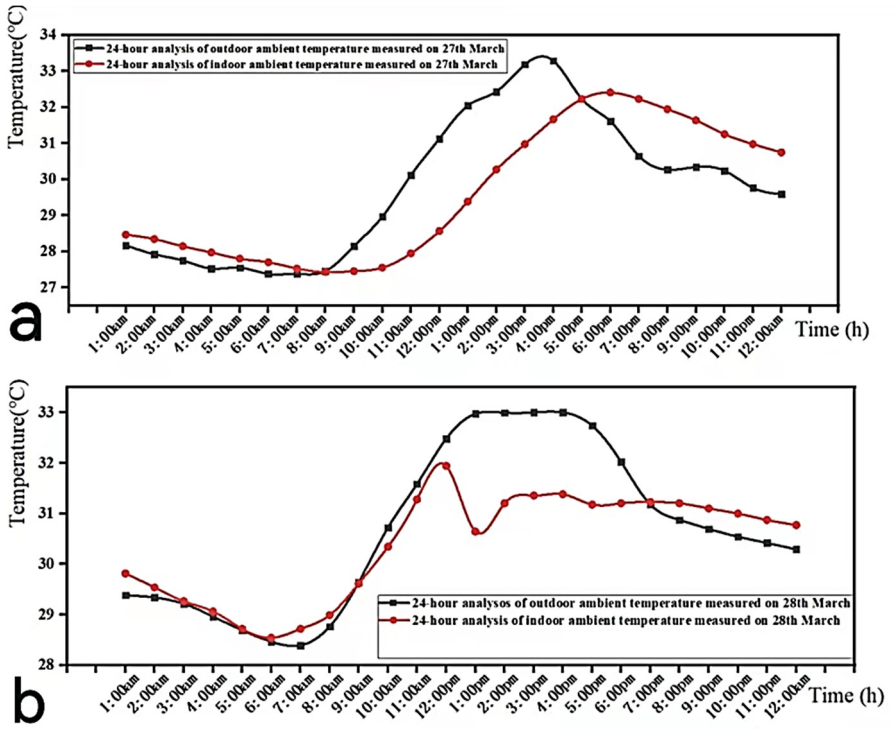

Fig. 8. The outdoor ambient temperature in 24 hours on 27th March 2022 measured: (a)on the 4th level; (b)on the 1st level at Room

March, 2022 and it is a good day without the influence of raining. Thus, we chose this day to do 24-hours systematic analysis. The outdoor ambient temperature starts to decrease at 1:00am and continued to plummet for the next 24 hours, reaching its lowest point at 8:00am, when it registers at 27.38°C. Then, the outdoor temperature rose rapidly and reached its highest point at 33.28°C at 5:00 pm on March 27, 2022. The average outdoor ambient temperature on this day is 29.74°C after a brief period of moderate temperature drop.

This research selected the minimum outdoor ambient temperature for analysis. As shown in Fig. 9, at 8:00 am on March 26, 2022, the outdoor ambient temperature as measured on level 4 fell to its lowest reading of 27.38°C, while the minimum value measured on level 1 was 25.86°C at the moment of 7:00am on 31 March, 2022. Then the ambient temperature fluctuated regularly. The temperature data from the 26th of March typically accurately reflected the lowest temperature situation.

Fig. 9 displays the outdoor ambient temperature data collected over a 24-hour analysis period. The analysis revealed that the lowest recorded temperatures occurred on two specific dates: the 26th of March 2022 in room A on the 4th level and the 31st of March 2022 in room B on the 1st level. As illustrated in Fig. 10, the indoor ambient temperature maintained at a relatively lower level of roughly 26.50°C at the beginning of the 24 hours, and leveled off a downward tendency. Then, it decreased to its minimum temperature of 27.43°C at the moment of 8:00am on 26th March, 2022. The value began to rise up and arrived at its maximum value of 30.46°C at the time of 3:00pm on 26th March 2022. Subsequently, it fell down again and declined to a relatively lower level. The average value of indoor ambient temperature was 28.76°C, which, when measured on the same floor, was lower than the ambient outdoor temperature.

As for the 1th level, the indoor ambient temperature kept a downward tendency and dropped to the bottom value of approximately 27.25°C, and then rocketed up and kept an upward tendency until 10:00pm. The highest indoor ambient temperature recorded on that day was greater than 29.50°C, and then after 10:00pm, the indoor ambient temperature dropped gradually. The maximum indoor ambient temperature measured on the 1st level is relatively lower than the value on the 4th level. Since the 4th floor of the

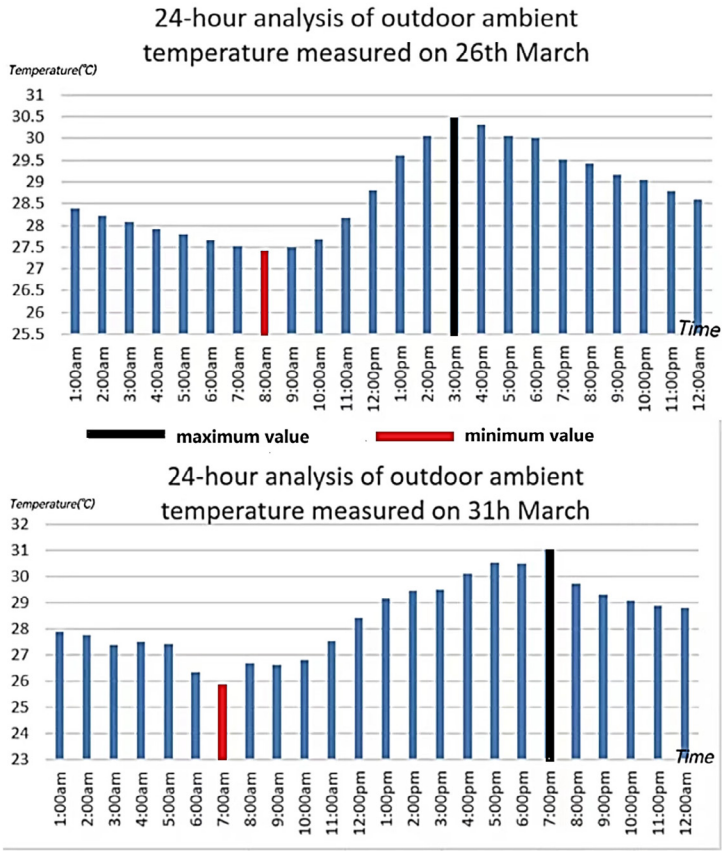

Fig. 9. The outdoor ambient temperature during the 24 hours analysis has indicated the minimum values measured on the 4th level room A on 26th March 2022 and on the 1st level room B on 31th March 2022

block was the highest, heat immediately entered through the roof. Even though the sunset occurred at 7:00 pm, heat continued to be transferred from the outdoor environment via the concrete wall and into the indoor space, increasing the temperature inside from 7:00 pm to 10:00 pm.

Wall Surface Temperature

Transmission electron microscopy (TEM) images of carbon nanotubes (CNTs) play a crucial role in understanding and controlling heat transfer in various applications. By utilizing TEM, the internal structure and characteristics of CNTs can be analyzed at the nanoscale level, providing valuable insights into their thermal conductivity and heat transfer properties. TEM images reveal the detailed morphology and atomic arrangement of CNTs, allowing for the observation of their individual walls, defects, and impurities. These images provide a deeper understanding of the structure-property relationship of CNTs and their role in heat transfer mechanisms. TEM analysis can reveal the presence of defects, such as vacancies, dislocations, or curvature, which can significantly influence the phonon scattering and thus affect the thermal conductivity of CNTs. By characterizing these defects, researchers can devise strategies to control and optimize the thermal properties of CNTs for efficient heat transfer applications. Furthermore, TEM images provide information about the interaction between CNTs and surrounding materials, such as polymers or metals, in composite systems. The interface between CNTs and the matrix material can be examined, allowing for the investigation of the thermal contact conductance and heat transfer pathways. These insights are crucial for designing materials with enhanced heat dissipation capabilities, where CNTs can act as efficient thermal bridges or pathways to facilitate heat transfer.

The maximum exterior surface temperature of the west wall was 36.41°C, and it peaked around

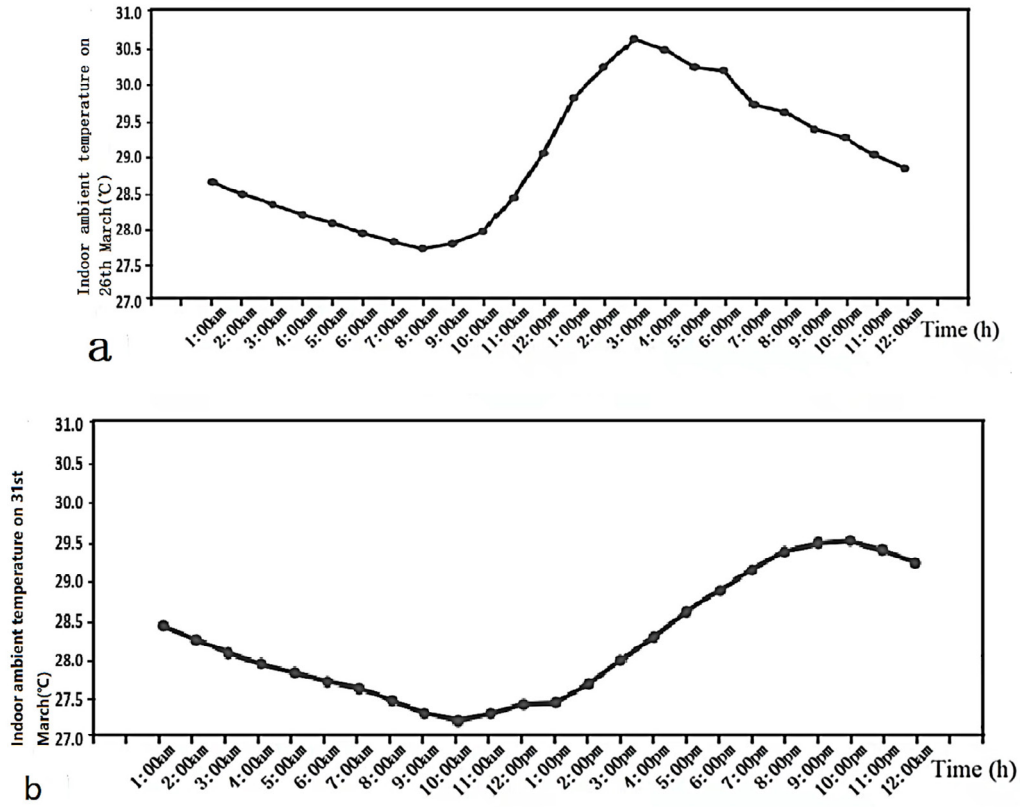

Fig. 10. The indoor ambient temperature in 24 hours measured: (a) on the 4th level on 26th March 2022; (b) on the 1st level on 31st March, 2022

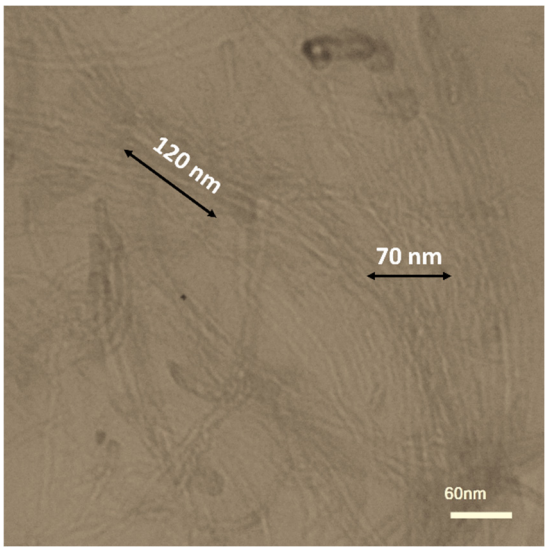

Fig. 11. TEM image of CNTs showcasing their internal structure and morphology

5:30 p.m. on 28th March 2022. Its value was substantially higher than the south wall's greatest exterior surface temperature, which reached to 32.72°C. The minimum external west wall surface temperature was 25.41°C, significantly lower than the lowest interior west. The two walls' average exterior surface temperature, which was roughly the same as one another at 29.15°C. As a residential

facade, solar radiation typically dominates passive cooling techniques, which are what define the thermal barrier performance of the RWH facade. As a result, the thermal gradient was created when the outer wall surface cooled and became colder than the interior, causing the heat to flow to the exterior, as shown in Fig. 12; passive cooling was achieved by heat dissipation and export.

To summarize, the surface temperature of the west wall was always higher than that of the east based on the comparison of the parameters, and the exterior surface temperature was always higher than the interior surface temperature based on the conduction heat transfer through the walls. In the 24-hour analysis, the external surface temperature of east wall was relatively higher only during the duration of 10am to 14pm with intense solar radiation, then the west wall surface temperature surpassed it and always remained a higher level on the whole. The surface temperature of external wall was much higher and fluctuated more dramatically than the internal, which had a temperature difference between the maximum and minimum value up to 13.24°C. The surface temperature of south wall indicated a subtle fluctuation tendency compared with the west and east walls. The average surface temperature of wall was always higher than the indoor ambient temperature. Fig. 13 depicts the average temperature of the external and internal surface temperature of the west and east walls. This is a comparative validation experiment which is conducted during 8th July to 15th July, and the yielded result strongly supported the fieldwork experiment results and data collection in March.

The reference case of the numerical investigation was used for experimental validation [28-31] to confirm the feasibility and cooling effectiveness of the RWH facade integration. Both Origin and HOBO software were used for data analysis and processing. Based on the result derived from Origin, the distribution trends were similar with an average deviation of 5.62%. The experiments were conducted with numerous uncertainties involving environmental conditions, climate characteristics, instrument precision, and operating errors [32].

Relative humidity

The average outdoor relative humidity was 73.43% during this measurement process, and its maximum value was 85.03% at the time of 7:56am on 26th March, as displayed in Fig. 14.

The average level of indoor relative humidity was 73.88%, which is nearly equal to the average of the outdoor relative humidity, and it rose up to the summit value of 84.96% at the time of 9:50am on 26th March, 2022.

Proposed RWH Facade & Heat Transfer Calculation

First and foremost, this research proposes the design of the RWH tank facade integrated with walls of different materials and its section, as shown in Figs. 15-16.

Proposed RWH Facade design

Fig. 15 showcases the proposed design of a RWH tank facade integrated with walls. The image presents a visual representation of the concept, illustrating how the RWH tank is seamlessly incorporated into the building's exterior walls.

The design aims to maximize space efficiency and aesthetic integration while allowing for the efficient collection and storage of rainwater. This

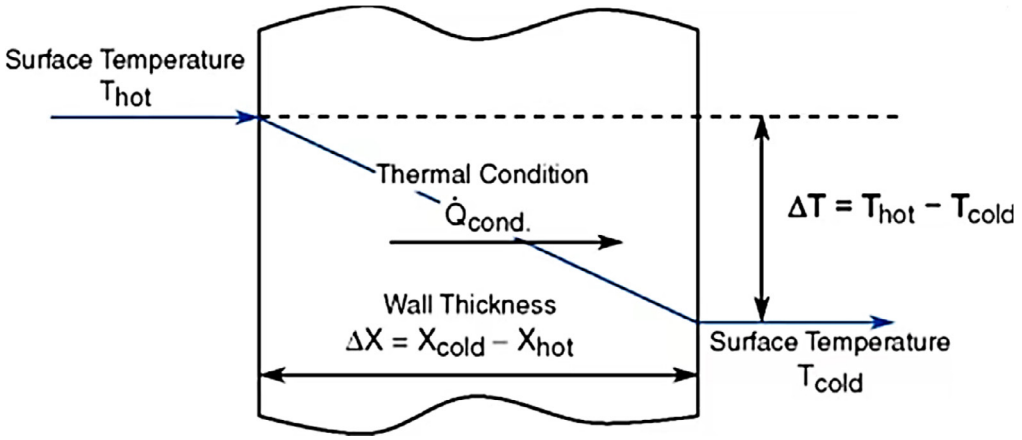

Fig. 12. The conduction heat transfer through the wall

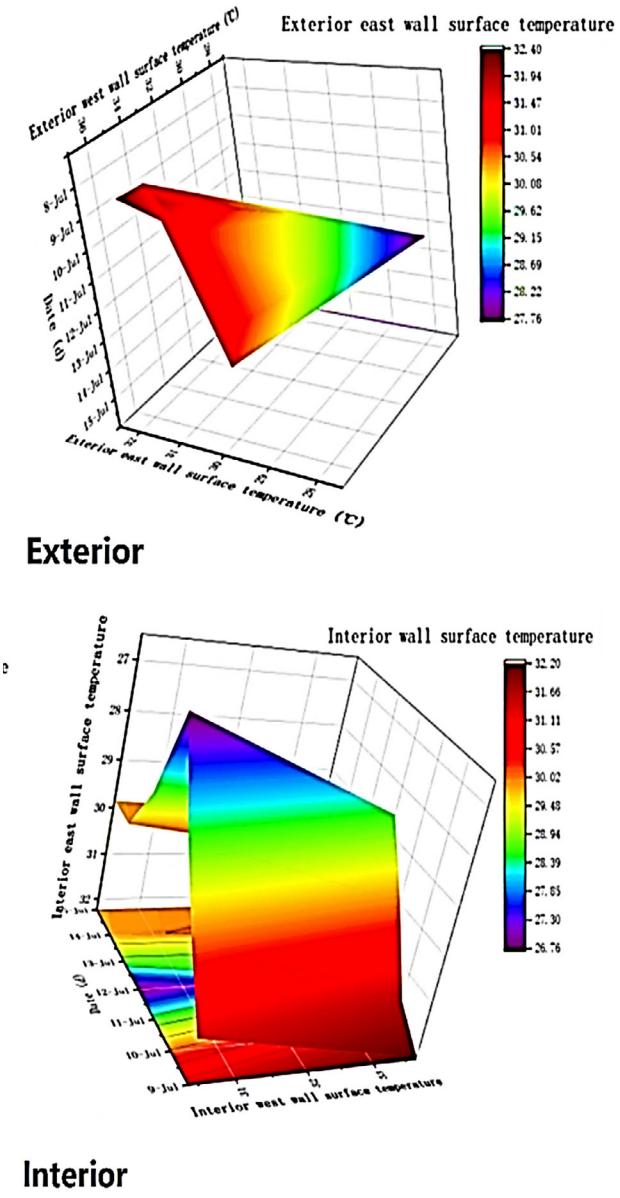

Fig. 13. The validation comparison of the exterior and interior surface temperature of the west and east walls

innovative approach offers potential benefits in terms of sustainable water management and resource conservation.

Fig. 16 provides a sectional view of the RWH facade. The image depicts a cross-section of the building, showcasing the specific details and components of the RWH system integrated into the facade. This section highlights the arrangement and configuration of the RWH tank, including its position within the building structure and the connection points for rainwater collection and distribution. By illustrating the internal workings of the RWH facade, this Fig. provides valuable insights into the functionality and implementation of this sustainable water management feature [33-39]. The ambient and surface temperatures under different experimental conditions were compared with and without the RWH facade to confirm the cooling effect of the RWH facade, combining the heat transfer calculation [40-45] to conclude the best thermal effect of reducing indoor temperature under different circumstances (with different wall materials such as reinforced concrete and brickwork), and optimizing the function of the

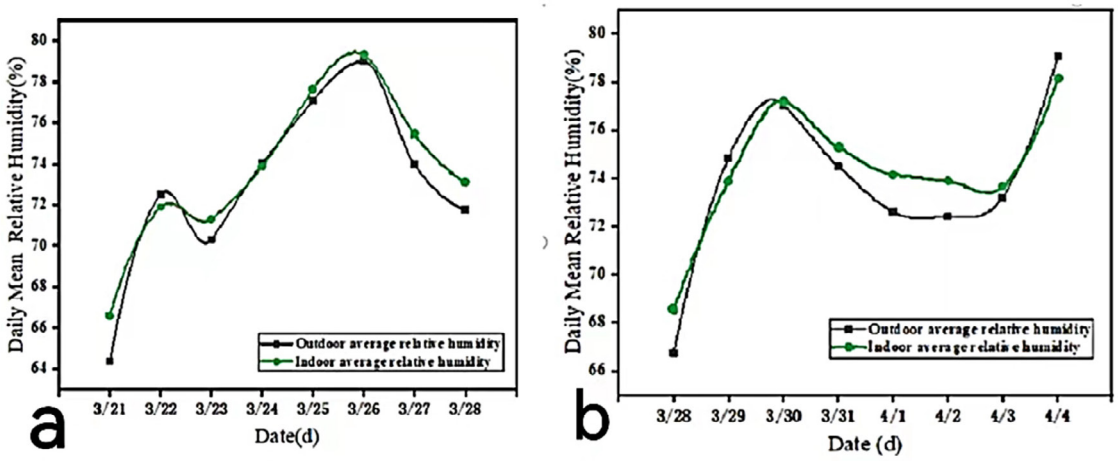

Fig. 14. The comparison and contrast of the relative humidity of the outdoor and indoor environment measured under two experimental conditions at Room 1

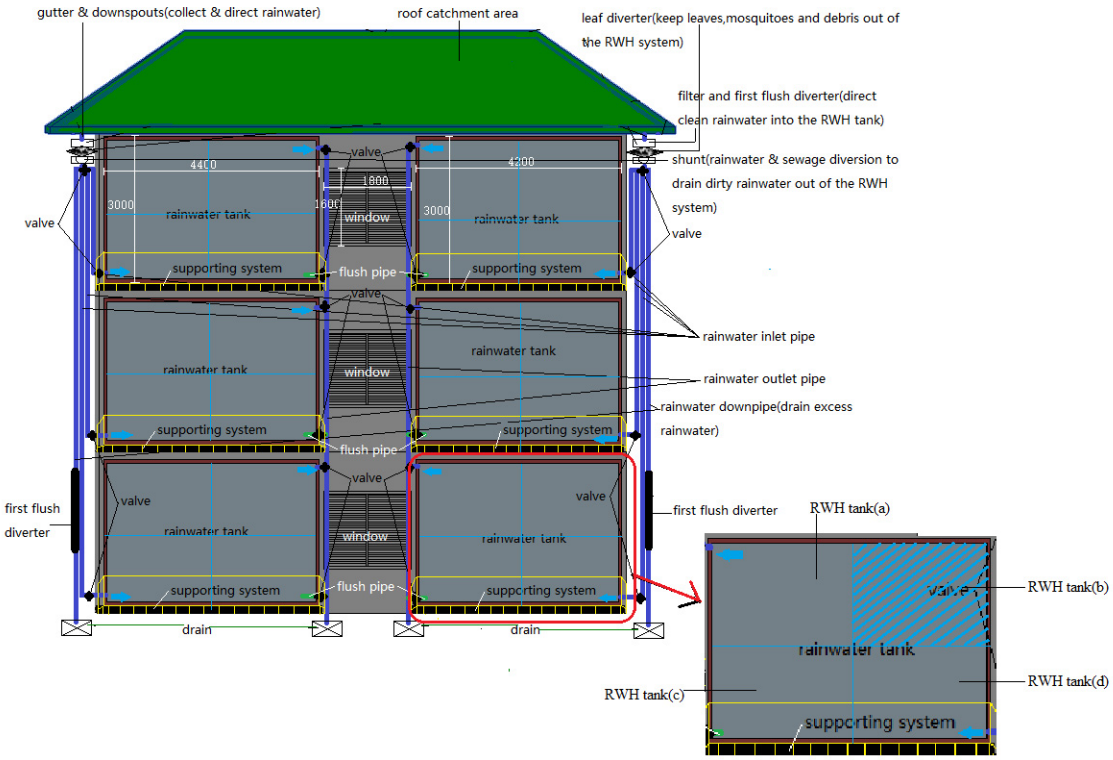

Fig. 15. Proposed design of RWH tank facade integrated with walls

RWH tank on the facade. There is the section and 3D model of the RWH facade design to simulate the heat transmission process, as illustrated in Figs. 17 and 18. The fact that heat and mass transfer are kinetic processes that can happen and be investigated both together and separately is a regular occurrence [40-42]. It is more effective to think about these two phenomena together since, in the case of conduction and convection (there is no mass-transfer similarity to heat radiation), both processes are characterized by comparable mathematical equations [43].

The study of heat and mass transfer involves examining the interplay between these processes,

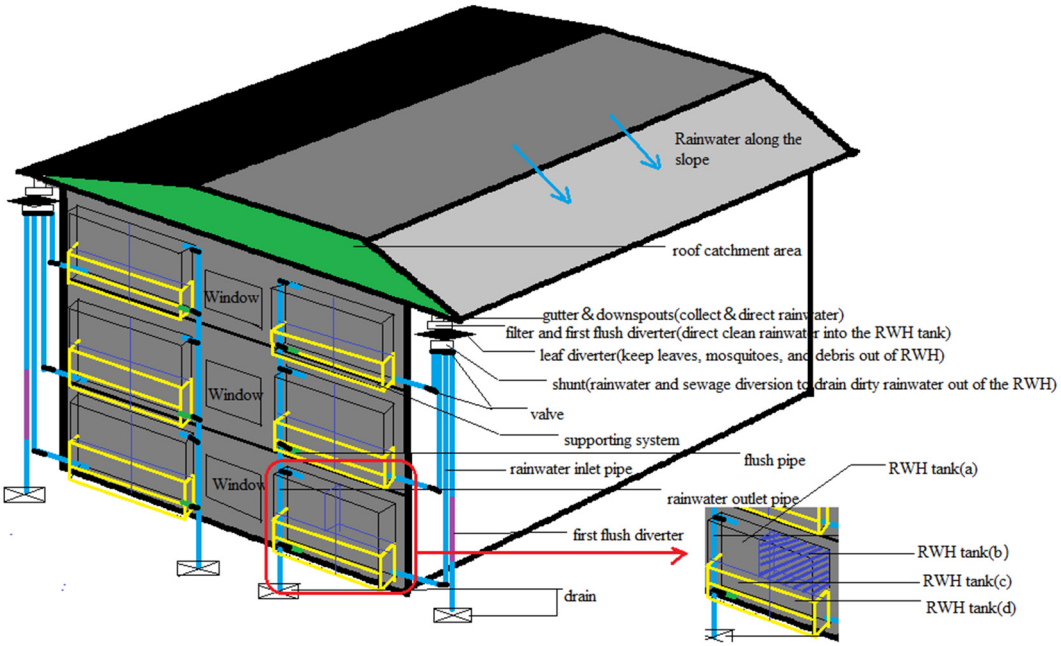

Fig. 16. The section of the RWH facade

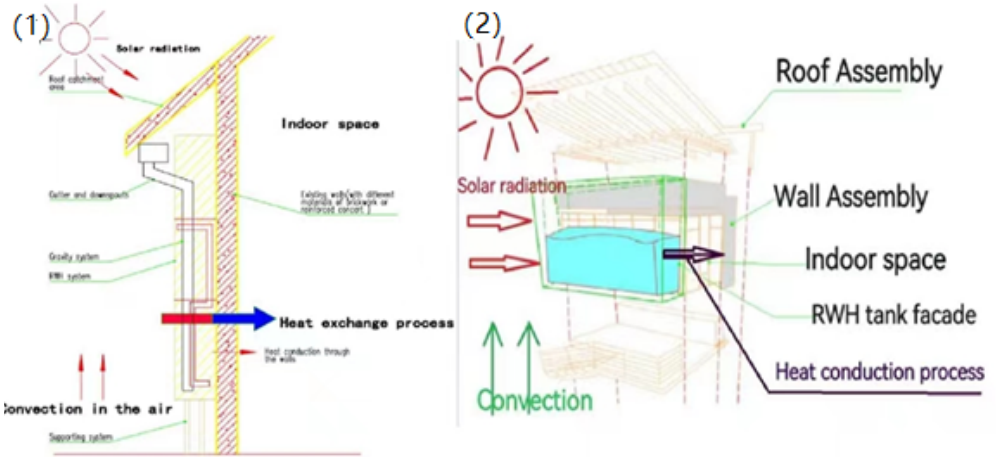

Fig. 17. Diagram 1 shows the installation of the RWH tank on the wall facade, while Diagram 2 illustrates the 3D model of heat transmission when integrated with RWH.

which can be investigated together or separately. However, it is often more effective to consider them together due to their interconnected nature. Fig. 18 displays the heat exchange process in the proposed design. The image provides a visual representation of how heat is transferred within the system, illustrating the flow of thermal energy and highlighting the key components involved in the exchange process.

Convective Heat Flux

The convective heat flux qc (W/m^2) is determined by the convective heat transfer coefficient "h" and the temperature difference between the air and the surface (Ta – Tw) according to Newton's cooling law [43-45]:

$$q_c = h \times \left(T_a - T_w\right) \text{ [45]}$$

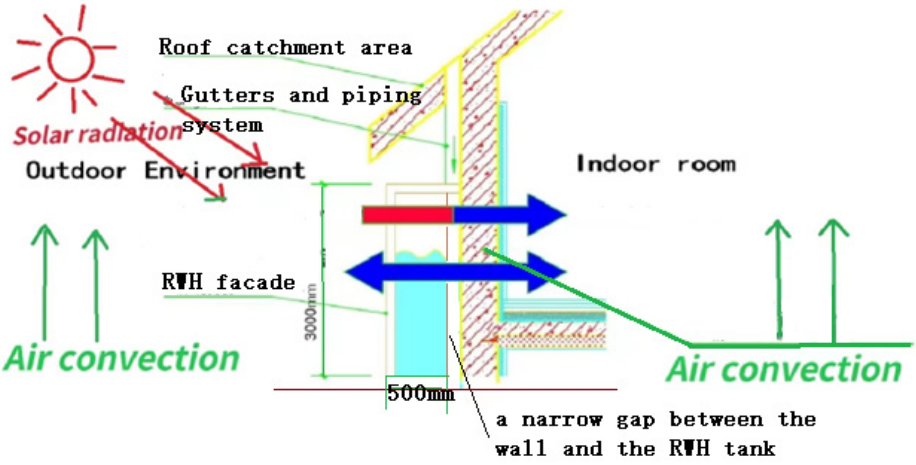

Fig. 18. Heat exchange process in the proposed design

where Ta is the air temperature, °C; Tw is the wall surface temperature, °C. Holman (J.P. Holman, Heat Transfer, 7th ed.) has given a simplified equation for the convective heat transfer coefficient between vertical surfaces and free flow of air at atmospheric pressure and moderate temperatures:

$$h = 1.42\sqrt[4]{\frac{\Delta T}{L}} \quad [45]$$

where $\Delta T = (Ta - Tw)$,°C

L = vertical dimension, m. The daily mean temperature of the wall surface is Tw, and the daily mean temperature of the air layer is Ta. That Tw is always lower than Ta suggests that the wall surface was gaining heat from the air layer all day, at an average convective heat flux. Similar analysis can be applied to the convective heat transfer from the air layer to the RWH tank. In this research, the daily average temperature of the exterior west wall surface is Tw = 29.106°C, and the daily average outdoor ambient temperature of the air is Ta = 29.292°C.
thus ΔT = 29.292°C–29.106°C =0.186°C; L = 3.0 m; therefore

$$qc = 1.42\sqrt[4]{\frac{\Delta T}{L}} = 0.708\ W/m^2$$

Tw is always lower than Ta, and the calculated results suggest that the west wall surface was gaining heat from the outdoor ambient air layer all day, at an average convective heat flux of 0.708W/m^2. And the daily average temperature of the exterior south wall surface was Tw = 29.254°C and the daily average outdoor ambient temperature of the air is Ta = 29.292°C.
thus ΔT = 29.292°C–29.254°C =0.038°C; L = 3.0 m; therefore

$$qc = 1.42\sqrt[4]{\frac{\Delta T}{L}} = 0.476 W/m^2$$

Because Tw is always less than Ta, the estimated results indicate that the south wall surface gained heat from the exterior ambient air layer all day, with an average convective heat flux of 0.476W/m^2. Similar analysis can be done for the convective heat transfer from the ambient air outside to the integration of the RWH tank and the existing walls. The integrated RWH tank on the residential facade and the wall surface both lose heat to the ambient outside air. It serves as the heat source for the RWH tank, existing walls, and the air microclimate.

Radiative Heat Flux

According to Holman, the net radiative heat flux (q_r) [45] between two parallel surfaces with the same size is

$$q_r = \frac{\sigma(T_1^4 + T_2^4)}{(1-\varepsilon_1)/\varepsilon_1 + 1/F_{1,2} + (1-\varepsilon_2)/\varepsilon_2} \quad [45]$$

where σ is the Stefan-Boltzmann constant with a value of 5.669 × 10−8 W/(m2 K4); T1 and T2 are the thermodynamic temperatures of the two surfaces, K; ε_1 and ε_2 are the emittance values of the two surfaces; $F_{1,2}$ is the radiation shape factor between the two surfaces. The surface with higher temperature loses more heat in emitting radiation than the radiation it absorbs from the other surface,

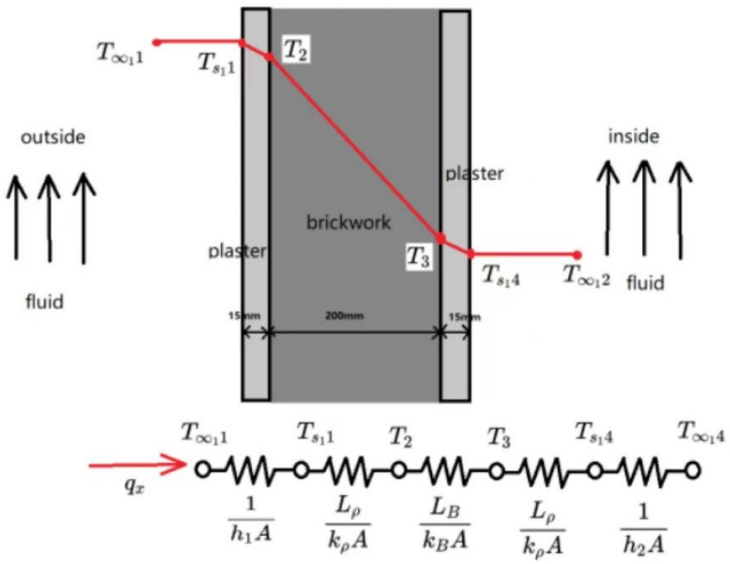

Fig. 19. Heat convection and conduction through wall layers of different materials

while it is vice versa for the surface with lower temperature [46]. In this research, the measured temperature of the exterior wall surface is always higher than the interior. Therefore, the exterior wall surface loses more heat in emitting to the interior wall surface than the heat it absorbs from it, even at night. The daily mean temperatures of the exterior and interior south wall surface temperatures are: T1=29.254℃=302.254K, T2=29.160℃=302.16K. The emittance value of the wall surface material (concrete) is $å_1$ =0.85, $å_2$ =0.85, which means that the wall is good at absorbing and emitting radiant heat. The shape factor $F_{1,2}$ = 1.0, based on the distance of the two surfaces and their sizes. And the constant σ is the Stefan-Boltzmann constant with a value of 5.669 × 10−8 W/ (m2 K4)

$$q_r = \frac{\sigma\left(T_1^4+T_2^4\right)}{(1-\varepsilon_1)/\varepsilon_1+1/F_{1,2}+(1-\varepsilon_2)/\varepsilon_2} = 0.46\text{W/ (m2 K4)}$$

The calculated result of q_r is 0.46W/ (m2 K4). The wall surface is cooled by the RWH tank on the residential college facade through radiative heat exchange. To summarize, the exterior wall surface gains heat from the outdoor ambient air and loses heat to the RWH tank system on the facade. The net heat loss of the south wall surface is q = qc- q_r =0.476-0.46=0.016W/m.

Increasing qc and/or decreasing q_r can remove more heat off the exterior wall surface, hence enhancing the cooling effect of the RWH tank integrated on the residential facade.

Conductive Heat Flux

Except for the heat transfer process of convection and solar radiation, heat is also transferred through the walls. The following physical formulas and deductive heat transfer equations [45] are used in this study to determine the conductive heat flux, as indicated in Fig. 19. In this study, in addition to convective heat transfer through air and water, heat conduction through solid walls also plays a role in the heat transfer from the outdoor environment to the internal space [45-46]. As a result, subject to the aforementioned presumptions, the thermal conductivity may be ascertained from Fourier's law in the calculation and data analysis process of this research.

In this study, we assume the steady-state, one-dimensional conduction, no internal heat regeneration, uniform heat transfer on exposed surfaces, and disregard corner and edge effects in the heat transfer process on the flat wall [45]. And with the classification of wall materials of three layers of plaster, brickwork, and plaster, we suppose that heat transfer occurs in three separate media. Other heat loads including internal load, transmission load, and infiltration load are not factored into calculations because they are believed to be constant. The following governing equations can be used to calculate heat transport based on the aforementioned presumptions. As a function

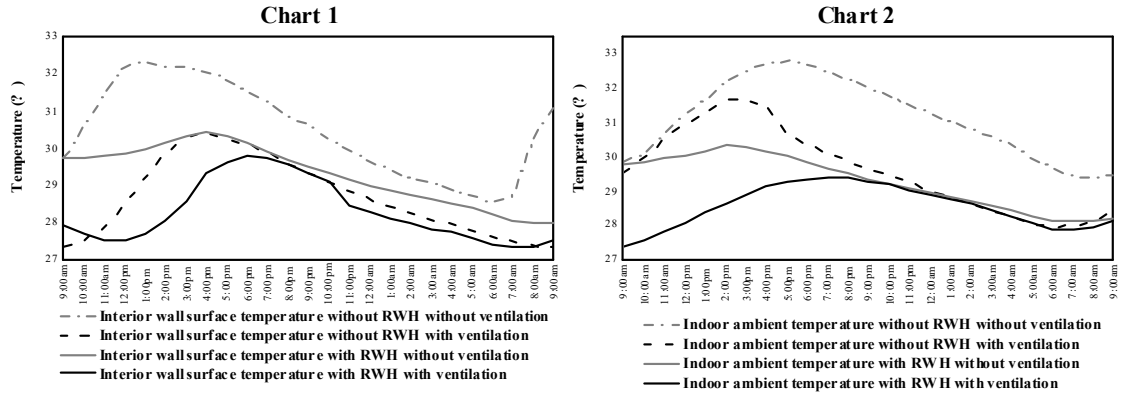

Fig. 20. Comparison and contrast between comprehensive experimental condition of installing the RWH tank with and without natural ventilation

of the ambient air temperatures within a range, heat loss occurs through the walls. The following parameters indicate the following meanings when these heat equations and formulas are applied to the calculation of heat and mass in this study: The term "qcond" refers to the quantity of thermal conductivity, "A" to the area of the wall, and "k" to the thermal conductivity of the wall's material. If "k" is just faintly temperature dependent, it is roughly constant [45]. Fourier's law provides the rate equation for conduction through the wall,

$$\frac{dQ}{dt} = \frac{k \times A \times \Delta T}{L} = \frac{A \times \Delta T}{\frac{L}{k}} \quad [45]$$

Namely, heat transfer in different medium and materials of plaster, brickwork, and plaster.

$$\frac{dQ}{dt} = \frac{A \times \Delta T}{\frac{L}{k}} = \frac{A \times \Delta T}{\frac{1}{h1} + \frac{Lp}{kp} + \frac{L_B}{k_B} + \frac{Lp}{kp} + \frac{1}{h2}} \quad [45]$$

Namely,

$$\frac{dQ}{dt} = \frac{A \times \Delta T}{R1 + Rp + RB + Rp + R2} \quad [45]$$

$$dT = T_1 - T_2 = \text{temperature gradient} - \text{difference} - \text{over the material } (^{\circ}C) \quad [45]$$

The R-value (thermal resistance) of the different material are illustrated as Rp, RB, and Rp.

$$\text{R-value (Resistance)} = \frac{\text{Thickness}}{\text{conductiviy}} \quad [45]$$

$$R_p = \frac{L_p}{k_p} \; ; R_B = \frac{L_B}{k_B} \; ; Rp = \frac{L_p}{k_p} \quad [45]$$

$$\text{Total thermal resistance: } R_{total} = \sum R_i = R_p + R_B + R_p \quad [45]$$

The reciprocal of R-value, U-value, or thermal transmittance, measure the rate of heat transmission through a structure (which may be made of a single material or a composite), divided by the temperature differential across that structure. W/m2K is used as the unit of measurement.

$$\text{Namely, U-value} = \frac{1}{R - \text{value}} \quad [45]$$

The calculation of heat transfer in this study takes into account the processes of heat convection of air and precipitation as well as the transmission of heat through walls. As a function of the ambient air temperatures within a range, heat loss occurs through the wall. When these heat equations and formulas are applied to heat and mass calculation in this research, the following parameters represent the following meanings: The thermal conductivity is measured in units of "qcond," "A," which represents the area of the wall, and "k," which stands for the material's thermal conductivity. "k" is roughly constant if its dependence on temperature is minimal.

The various heat transfer layers are depicted in Fig. 16, and they include two layers of plaster, brickwork layer, and air fluid. Air has a thermal conductivity of 0.026 W/m K, while the value of plaster is 0.40 W/m K, and water has a thermal conductivity of 0.6 W/m K. The thermal

conductivity of a block is 1.31 W/m K due to the brickwork that makes up its outside wall. For example, "h_1" stands for the thermal conductivity of air, while "h_2" denotes the thermal conductivity of water.

The total thermal resistance:

$$\text{Rtotal} = \sum R_i = \frac{1}{h_1 \times A} + \frac{L_p}{k_p \times A} + \frac{1}{h_2 \times A} + \frac{L_p}{k_p \times A} + \frac{1}{h_1 \times A}$$ [45]

Heat flux:

$$qx'' = \frac{\Delta T}{\text{Rtotal}} = \frac{(T1 - T2)}{\frac{1}{h_1 \times A} + \frac{Lp}{kp \times A} + \frac{1}{h_2 \times A} + \frac{Lp}{kp \times A} + \frac{1}{h_1 \times A}}$$ [45]

Thermal transmittance:

$$\text{U-value} = \frac{1}{\text{R} - \text{value}} = \frac{1}{\text{Rtotal}}$$ [45]

This research can find the predicted temperature and temperature reduction under the condition of installing the rainwater tank on the residential college facade to confirm that installing rainwater tank as facade has a considerable potential to lower the indoor temperature and increase occupant thermal comfort. As for the calculation of heat transfer through the plane walls, this research conducts these assumptions: temperature variation occurring only through the wall, depth-wise; the corner and edge effects were ignored, and uniform heat transfer on the expected surface was assumed. No heat regeneration during the heat transfer process was considered and steady state was maintained [45]. By substituting numerical values, heat transfer was calculated on the east wall.

This study determines the heat transmission through the existing walls as well as their U-value and R-value based on the wall surface temperature measured during the onsite case study [45-46]. The expected indoor ambient temperature and predicted temperature reduction were then calculated by combining the outdoor and indoor ambient temperatures recorded during the case study with the thermal conductivity of the various materials, which is in the room whose proposed walls made of different materials, namely plaster and brickwork [46]. As an illustration, the outside west wall surface temperature in group 1 calculations is 37.340°C, or T1, while the internal west wall surface temperature is 31.870°C, or T2. Heat is transferred through conduction through the west wall and convection in the air before entering the block's interior. Air has a thermal conductivity of 0.026 W/m K, while a dense brick wall has a value of 1.31 W/m K. The west wall is 0.15 meters thick, or L=0.15 meters. The west wall's measured area is 1.65m*3m, or 4.95m2. In addition to heat conduction through the wall, the heat transfer via the west wall also involves the processes of heat convection through water and air.

The total thermal resistance:

$$\text{Rtotal} = \sum R_i = \frac{1}{h_1 \times A} + \frac{L_p}{k_p \times A} + \frac{1}{h_2 \times A} + \frac{L_p}{k_p \times A} + \frac{1}{h_1 \times A}$$

$$= 1/(0.026\text{W/m·K}*4.95\text{m2}) + 0.15\text{m}/(0.40\text{W/m·K}*4.95\text{m2}) + 1/(0.6\text{W/m·K}*4.95\text{m2}) + 0.15\text{m}/(1.31\text{W/m·K}*4.95\text{m2}) + 1/(0.026\text{W/m·K}*4.95\text{m2}) = 1.8343\text{Km}^2\text{/W}$$

$$\text{Heat flux: } qx'' = \frac{\Delta T}{\text{Rtotal}} = \frac{(T1 - T2)}{\frac{1}{h_1 \times A} + \frac{Lp}{kp \times A} + \frac{1}{h_2 \times A} + \frac{Lp}{kp \times A} + \frac{1}{h_1 \times A}}$$

$$= (37.340°\text{C} - 31.870°\text{C})/1.6021\text{Km}^2\text{/W} = 2.98\text{W}$$

Thermal transmittance:

$$\text{U-value} = \frac{1}{\text{R} - \text{value}} = \frac{1}{\text{Rtotal}} = 0.55\text{W/m}^2\text{K}$$

Namely, in the calculation of this group data, the thermal transmittance of the west wall is 0.55W/m²K, which equals to the U-value of the west wall. We may infer that installing a rainwater tank on the residential college's facade has a significant impact on lowering the relative humidity in the interior space and improving the thermal comfort of the residents [24,46-48]. Both the exterior and interior surface with RWH has a much smaller temperature fluctuation comparing to the bare wall facade without RWH, as shown in Figs. 20, 21, and 22.

Owing to the factor of orientation, the west wall of block receives more intense solar radiation compared with other walls, and its surface temperature is relatively higher, and we choose the exterior and interior surface temperature to get more distinct fluctuation difference. The overall exterior wall surface temperature with the RWH tank on the facade is cooler by a maximum of 14.41°C comparing to the bare facade wall without the RWH tank. The exterior west wall surface with the RWH tank is cooler by a maximum of 3.41°C comparing to the other series maximum west wall surface temperature without the RWH tank while the interior wall surface is cooler by a maximum of 1.80°C. The ambient temperature of indoor dormitory room is reduced at a maximum of 1.54°C, and the average temperature of the indoor dormitory room is 0.81°C less than the

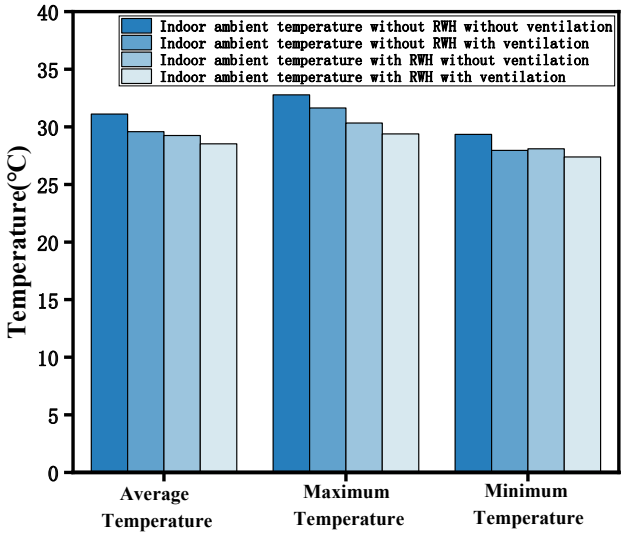

Fig. 21. The comparison and contrast of the indoor ambient temperature measured under two different experimental condition with windows closed and open in two series experiment

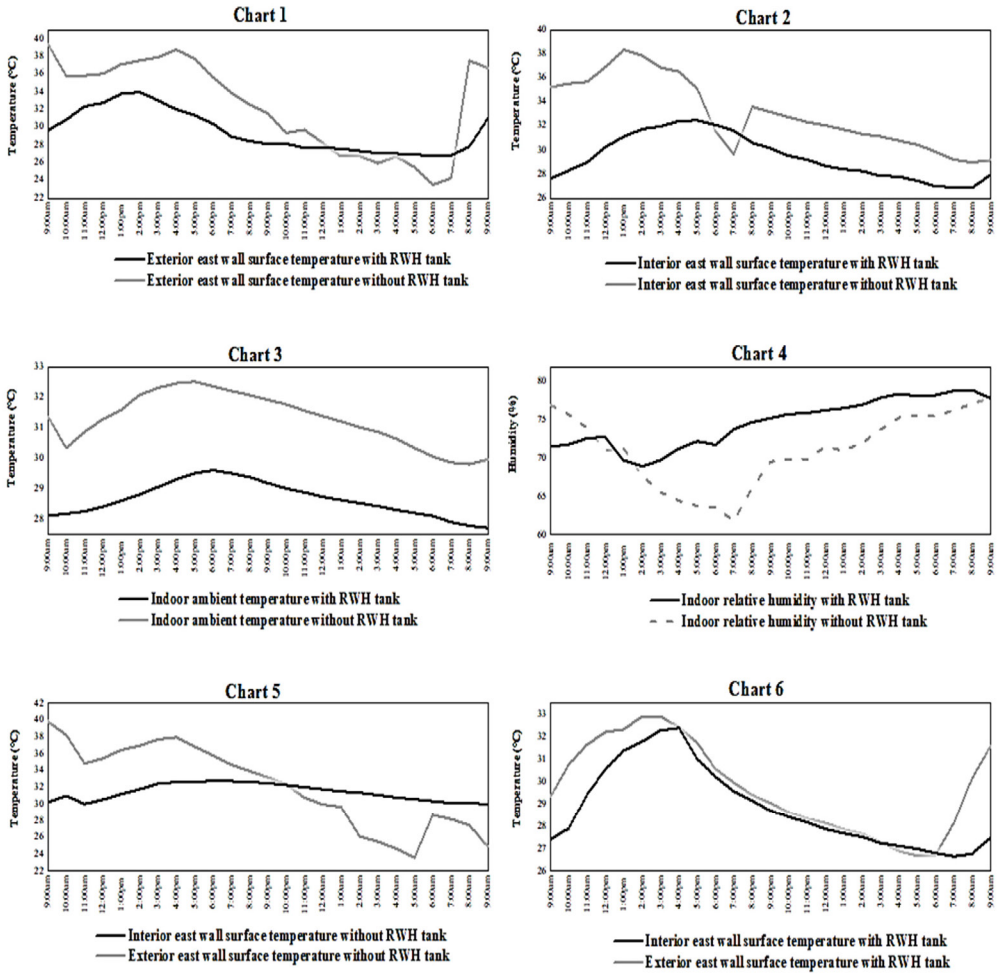

Fig. 22. Comparison between the bare wall without RWH tank and with RWH tank on the façade

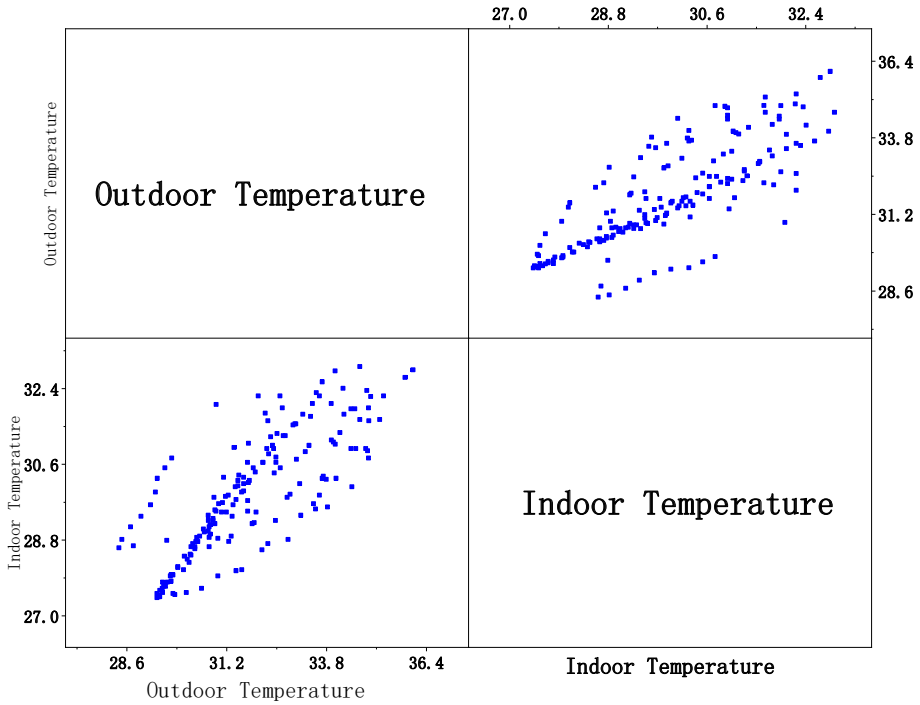

Fig. 23. Matrix scatter plot showing I/O ratio

space without the RWH tank on the residential college facade. Chart 1 in Fig. 20 illustrates the exterior surface temperature of the west wall under the experimental condition with and without the RWH facade. It is clear that the bare west wall gains heat during the daytime since the exterior surface temperature is always higher than the interior surface temperature, and it releases heat to the ambient air at night. However, the wall integrated with the RWH tank on the facade manifested a different feature [49]. The fluctuation tendency of exterior surface temperature with the RWH tank is not so dramatic. Compared with the other series experiment, the exterior west wall surface temperature with RWH facade on the residential college facade is relatively lower.

It is safe to conclude the constant north-south airflow in the dormitory rooms, which is caused by the experimental circumstance of leaving the windows open. This natural ventilation and breeze provide passive cooling, which causes the west and south walls' internal surface temperatures to be nearly identical, and the indoor ambient temperature measured on the higher level is higher than the Fig. recorded on the lower level [49-51].

The interior wall surface temperature and the indoor ambient temperature shown as chart 2 and chart 3 also have a similar tendency. The block with RWH facade shows a relatively lower temperature, and the bare wall without RWH demonstrated a more drastic temperature fluctuation tendency. The temperature amplitude (the absolute value of the maximum difference between the alternating temperatures from its mean value) of the interior wall surface with the RWH facade is 3.02℃, 39.6% smaller than the other interior wall surface without RWH, whose temperature amplitude is 5.37℃. This is the result of having a smaller impact on the heat transfer through the wall. Chart 3 shows that the indoor ambient temperature of both dormitory rooms with and without RWH, which also have a different fluctuation range. The temperature amplitude of the indoor air with the RWH tank is 0.96℃, 22.6% smaller than the other series experiment without RWH, whose temperature amplitude is 1.236℃. The average indoor ambient temperature with RWH is 28.65℃ and the other series without RWH is 31.27℃. The RWH facade has a promising effect on cooling the indoor environment and stabilizing the wall surface temperature.

As depicted in Chart 4 of Fig. 22, the indoor relative humidity levels in the dormitory are noticeably lower without the RWH system

compared to when the RWH system is implemented, both during the day and at night. The impact of the RWH system on indoor humidity appears to be relatively limited. These findings suggest that the RWH tank contributes to a more stable relative humidity environment in the dormitory room, with only slight fluctuations observed [48-50]. This study defines the temperature I/O ratio (the ratio of indoor ambient temperature to outdoor ambient temperature) as the decrement factor in order to analyze the variation fluctuation and difference between the outdoor and indoor ambient temperatures measured near the wall of the dormitory dwelling, as well as to evaluate the passive cooling effect of the RWH facade system. Fig. 23 displays the calculation results and trend analysis, and the analysis is carried out in accordance with the results. It was discovered that the two sets of data from the two levels' experiment tested had similar fluctuation tendency. By calculating the experimentally measured data, this study discovered that the I/O ratio was lower during the noon period (11am-4pm) when the solar radiation was strongest. And through the calculation, the I/O ratio of the calculated proposed design integrated with the RWH facade is lower than the measured existing wall. In addition, this research also indicated the variation of surface temperature and heat flow of proposed RWH integration and existing walls.

RWH in student residential colleges has the potential to enhance internal temperature control and improve occupants' comfort. By integrating RWH systems into the building's facade, the tanks can act as a thermal buffer, reducing heat transfer and regulating indoor temperatures. This study investigates the effectiveness of retrofitting RWH tanks in a case study area. The collected data, including ambient temperature, wall surface temperature, and relative humidity, demonstrate a linear correlation between the installation of RWH tanks and the reduction of indoor temperature. The findings suggest that retrofitting RWH tanks can significantly contribute to the passive cooling of student residential colleges. These findings have implications for sustainable building design and can inform future retrofitting strategies to optimize energy efficiency and occupant comfort in educational institutions. As for the effect on installing rainwater tank on the RWH facade, the data of indoor and outdoor ambient temperature, interior and exterior wall surface temperature, and relative humidity were collected and analyzed in the case study area. The data reveal a liner correlation between installing rainwater tanks on the residential college' facade and reducing indoor temperature as well as improving occupants' thermal comfort and sensation. The results clearly indicate that the installation of rainwater tanks on the facade is the main factor of the reduction of the indoor temperature and improve thermal comfort. To summarize, the heat exchange process occurs inside the microclimate of case study in this research, where the heat transfer process of convection, conduction, and radiation are all present. Wall insulation mainly resists the amount of heat conduction and convection, which provides insulation and less heat absorbance inside the building due to their ability to reflect solar irradiance [46]. It can be achieved using different kinds of materials. As for the dormitory rooms, even though radiation and convection occur in conjunction with each other, convective and radiative heat fluxes are independent of one another, can be calculated independently, and may simply be added. Therefore, the net heat loss of the wall surface is the sum of the heat exchanged from convection and radiation [46]. Considering different wall assembly constructions beyond a single composition is crucial in order to enhance the applicability and generalizability of the research results. Walls in real-world scenarios are often constructed using various materials and configurations, and their thermal performance can vary significantly based on these factors. By exploring a range of wall assembly constructions, the research findings can provide more comprehensive insights into the effectiveness of passive cooling strategies and their applicability in different contexts. The inclusion of diverse wall compositions allows for a broader understanding of how different materials and configurations impact heat transfer and thermal comfort [50-51].

CONCLUSIONS

Incorporating carbon-based materials into building components can enhance their energy-saving capabilities. Carbon-based insulation materials can be employed to minimize heat transfer through walls, roofs, and floors, effectively reducing energy requirements for heating and cooling. Moreover, carbon-composite panels or facades can be utilized to improve thermal insulation, contributing to better energy

efficiency and indoor comfort. Carbon-based materials demonstrate promising characteristics for preventing energy loss in walls. Moreover, their excellent thermal conductivity, lightweight nature, and compatibility with building materials make them a valuable resource for sustainable construction. By incorporating these materials into building components, we can contribute to energy conservation efforts and create more environmentally friendly and energy-efficient structures. Retrofitting rainwater collection systems involves the integration of tanks or storage units into existing structures to capture and store rainwater, enabling its reuse for irrigation, toilet flushing, and cooling systems. This approach reduces reliance on conventional water sources and eases the burden on municipal water supplies, conserving water resources and enhancing resilience in the face of water scarcity and climate change. An analysis of RWH facades using statistical and quantitative methodology has identified ambient and surface temperature, as well as relative humidity, as significant factors that influence heat flux through walls and facilitate indoor passive cooling. Through two series of experiments in a tropical climate, this research investigated the thermal behavior of the RWH system, focusing on the thermal properties of the microclimate between the wall surface and the RWH facade. The study calculated heat transfer, U-value, and R-value of walls, predicted indoor temperatures with different wall materials, and compared the proposed RWH-integrated residential college to an existing structure to confirm the thermal properties and cooling effects of the RWH system. Key findings include: (1) The addition of an RWH tank to the residential college facade resulted in significant cooling effects, with maximum temperature reductions of 14.41°C on the exterior wall surface, 3.41°C on the exterior west wall surface, 1.80°C on the interior wall surface, and an average ambient temperature reduction of 0.80°C in the interior dorm. Cooling effects were more pronounced on exterior surfaces. (2) The RWH facade acted as a thermal barrier, absorbing less solar radiation and minimizing heat transfer from the external to the internal environment, thereby reducing indoor temperatures. (3) The microclimate between the RWH facade and the wall exhibited cooler air compared to the ambient air. The RWH tank served as a passive cooling strategy, extracting heat from the air and wall surface, while the ambient air acted as the heat source, bringing in heat from the surroundings. (4) Bare walls without RWH experience higher solar radiation absorption, affecting the indoor thermal comfort of the residential college. This confirms the significance of passive cooling and heat transfer in the study. (5) The exterior wall surface lost heat to the microclimate through a combination of convective and radiative heat exchange, resulting in reduced temperature fluctuations and heat flux. (6) The RWH tank had only a minimal impact on indoor humidity, slightly increasing the mean relative humidity (RH) in the dormitory room. As the air layer directly influenced the wall surface, indoor humidity remained relatively unchanged.

ACKNOWLEDGMENTS

Authors would like to thank Faculty of Built Environment, University of Malaya for sponsoring this work.

CONFLICTS OF INTEREST

The authors declare no conflict of interest.

REFERENCES

1. Hassan WH, Hussein HH, Nile BK. The effect of climate change on groundwater recharge in unconfined aquifers in the western desert of Iraq. Groundwater for Sustainable Development. 2022;16:100700.
2. Chophel Y. Global Warming and Climate Change (GWCC) Realities. The Nature, Causes, Effects and Mitigation of Climate Change on the Environment. 2022:3.
3. Kubota T, Hooi S, Remaz DCT. Energy consumption and air-conditioning usage in residential buildings of Malaysia. Journal of International Development and Cooperation. 2011;17:61-9.
4. Gwoździej-Mazur J, Jadwiszczak P, Kaźmierczak B, Kózka K, Struk-Sokołowska J, Wartalska K, et al. The impact of climate change on rainwater harvesting in households in Poland. Applied Water Science. 2022;12(2):15.
5. Fanger PO. Thermal comfort. Analysis and applications in environmental engineering.244 pp.
6. Imteaz MA, Shanableh A, Rahman A, Ahsan A. Optimisation of rainwater tank design from large roofs: A case study in Melbourne, Australia. Resources, Conservation and Recycling. 2011;55(11):1022-9.
7. Tuck NW, Zaki SA, Hagishima A, Rijal HB, Zakaria MA, Yakub F. Effectiveness of free running passive cooling strategies for indoor thermal environments: Example from a two-storey corner terrace house in Malaysia. Building and Environment. 2019;160:106214.
8. Venkiteswaran VK, Lern WD, Ramachanderan SS. A Case Study on the Use of Harvested Rainwater to Operate Passive Cooling Water Wall (PCWW) for SEGi University Tower. Energy Procedia. 2017;105:419-26.
9. Imessad K, Derradji L, Messaoudene NA, Mokhtari F, Chenak A, Kharchi R. Impact of passive cooling techniques on energy demand for residential buildings in a Mediterranean climate. Renewable Energy. 2014;71:589-97.

10. Mohammed T, Megat Mohd Noor MJ, Megat Mohd Noor MJ, Noor A, Ghazali A. Study on Potential Uses of Rainwater Harvesting in Urban Areas. 2006.
11. JL A, Bolong N, Makinda J. Feasibility study of rainwater harvesting in Universiti Malaysia Sabah's residential colleges in support of the eco-campus initiative. Journal of BIMP-EAGA Regional Development. 2015;1(1):1-9.
12. Shaari N, Ani AIC, Nasir N, Zain MFM, Fui GS. Rainwater Harvesting: Potential for Quality Living. Icbedc; 2008.
13. Aghandeh P, Kouhestani F, Isamorad F, Akbari S, Tanbakuchi B, Motamedian SR. Efficacy of Application of Periodontal Ligament Stem Cells in Bone Regeneration: A Systematic Review of Animal Studies. Dental Hypotheses. 2022;13(4):111-6.
14. Zaidan SM, Rafeeq RA. Comparison of shear bond strength of three luting materials used in band and loop space maintainer cementation: an in vitro study. Dental Hypotheses. 2022;13(4):136-8.
15. Kadhem DJ, Al Haidar AHM. Remineralization of dentine caries using moringa oleifera based nano-silver fluoride: a single-blinded, randomized, active-controlled clinical trial. Dental Hypotheses. 2022;13(3):82-5.
16. Fanger PO. Assessment of man's thermal comfort in practice. British journal of industrial medicine. 1973;30(4):313-24.
17. Ricciardi P, Buratti C. Thermal comfort in open plan offices in northern Italy: An adaptive approach. Building and Environment. 2012;56:314-20.
18. Franz DJ. Quantitative research without measurement. Reinterpreting the better-than-average-effect. New Ideas in Psychology. 2023;68:100976.
19. Matović N, Ovesni K. Interaction of quantitative and qualitative methodology in mixed methods research: integration and/or combination. International Journal of Social Research Methodology. 2023;26(1):51-65.
20. Rouleau G, Hong QN, Kaur N, Gagnon MP, Côté J, Bouix-Picasso J, et al. Systematic Reviews of Systematic Quantitative, Qualitative, and Mixed Studies Reviews in Healthcare Research: How to Assess the Methodological Quality of Included Reviews? Journal of Mixed Methods Research. 2021;17(1):51-69.
21. Mariani MM, Machado I, Nambisan S. Types of innovation and artificial intelligence: A systematic quantitative literature review and research agenda. Journal of Business Research. 2023;155:113364.
22. Qi L, Han G, Jiang Z. Optimal design of E-type coaxial thermocouples for transient heat measurements in shock tunnels. Applied Thermal Engineering. 2023;218:119388.
23. Moscoso-García P, Quesada-Molina F. Analysis of Passive Strategies in Traditional Vernacular Architecture. Buildings [Internet]. 2023; 13(8).
24. Vox G, Blanco I, Schettini E. Green façades to control wall surface temperature in buildings. Building and Environment. 2018;129:154-66.
25. Blanco I, Schettini E, Scarascia Mugnozza G, Vox G. Thermal behaviour of green faÃ§ades in summer. Journal of Agricultural Engineering. 2018;49(3):183-90.
26. Blanco I, Convertino F, Schettini E, Vox G. Wintertime thermal performance of green façades in a Mediterranean climate. Urban Agriculture City Sustainability II. 2020;243:1147.
27. Campiotti CA, Gatti L, Campiotti A, Consorti L, De Rossi P, Bibbiani C, et al. Vertical Greenery as Natural Tool for Improving Energy Efficiency of Buildings. Horticulturae [Internet]. 2022; 8(6).
28. Madushika U, Ramachandra T, Zainudeen N. Operational energy saving in buildings: a comparison of green vs conventional wall. 2021.
29. Ako AA, Nzali CT, Lifongo LL, Nkeng GE. Rainwater harvesting (RWH): a supplement to domestic water supply in Mvog-Betsi, Yaoundé-Cameroon. Water Supply. 2021;22(1):1141-54.
30. Bolhari A, Castaneda DI, Arehart JH, Tillema SJ. Performance analysis and life cycle assessment of acrylic concrete structures for rainwater harvesting. Resources, Conservation & Recycling Advances. 2022;13:200063.
31. Han D, Ng BF, Wan MP. Preliminary study of passive radiative cooling under Singapore's tropical climate. Solar Energy Materials and Solar Cells. 2020;206:110270.
32. Rahman A. Rainwater Harvesting for Sustainable Developments: Non-Potable Use, Household Irrigation and Stormwater Management. Water [Internet]. 2021; 13(23).
33. Christian Amos C, Rahman A, Mwangi Gathenya J. Economic Analysis and Feasibility of Rainwater Harvesting Systems in Urban and Peri-Urban Environments: A Review of the Global Situation with a Special Focus on Australia and Kenya. Water [Internet]. 2016; 8(4).
34. GhaffarianHoseini A, Tookey J, GhaffarianHoseini A, Yusoff SM, Hassan NB. State of the art of rainwater harvesting systems towards promoting green built environments: a review. Desalination and Water Treatment. 2016;57(1):95-104.
35. Peker E. Enabling widespread use of rainwater harvesting (RWH) systems: challenges and needs in twenty-first-century Istanbul. European Planning Studies. 2023;31(1):103-22.
36. Istchuk RN, Ghisi E. Influence of Design Variables on the Financial Feasibility of Rainwater Harvesting Systems. Water [Internet]. 2023; 15(6).
37. Istchuk RN, Ghisi E. Influence of rainfall time series indicators on the performance of residential rainwater harvesting systems. Journal of Environmental Management. 2022;323:116163.
38. Ghosh S, Ahmed T. Assessment of Household Rainwater Harvesting Systems in the Southwestern Coastal Region of Bangladesh: Existing Practices and Household Perception. Water. 2022; 14(21).
39. Fonseca L, Olmeda P, Novella R, Valle RM. Internal Combustion Engine Heat Transfer and Wall Temperature Modeling: An Overview. Archives of Computational Methods in Engineering. 2020;27(5):1661-79.
40. Ghadirinejad N, Ghadiri Nejad M, Alsaadi N. A fuzzy logic model and a neuro-fuzzy system development on supercritical CO2 regeneration of Ni/Al2O3 catalysts. Journal of CO_2 Utilization. 2021;54:101706.
41. Al-Sanea SA. Evaluation of Heat Transfer Characteristics of Building Wall Elements. Journal of King Saud University - Engineering Sciences. 2000;12(2):285-312.
42. Iwaro J, Mwasha A. Effects of Using Coconut Fiber–Insulated Masonry Walls to Achieve Energy Efficiency and Thermal Comfort in Residential Dwellings. Journal of Architectural Engineering. 2019;25(1):04019001.
43. Ghasemi M, Nejad MG, Alsaadi N, Abdel-Jaber Mt, Ab Yajid MS, Habib M. Performance Measurment and Lead-Time Reduction in EPC Project-Based Organizations: A Mathematical Modeling Approach. Mathematical Problems in Engineering. 2022;2022:5767356.

44. Lei J, Yang J, Yang E-H. Energy performance of building envelopes integrated with phase change materials for cooling load reduction in tropical Singapore. Applied Energy. 2016;162:207-17.
45. Holman JP. Heat Transfer. 2010;10th Edition.
46. Davani PP, Kloub AWM, Ghadiri Nejad M. Optimizing the first type of U-shaped assembly line balancing problems. Annals of Optimization Theory and Practice. 2020;3(4):65-82.
47. Rabani M, Kalantar V, Dehghan AA, Faghih AK. Empirical investigation of the cooling performance of a new designed Trombe wall in combination with solar chimney and water spraying system. Energy and Buildings. 2015;102:45-57.
48. Radhakrishnamacharya G, Srinivasulu C. Influence of wall properties on peristaltic transport with heat transfer. Comptes Rendus Mécanique. 2007;335(7):369-73.
49. Wong NH, Kwang Tan AY, Chen Y, Sekar K, Tan PY, Chan D, et al. Thermal evaluation of vertical greenery systems for building walls. Building and Environment. 2010;45(3):663-72.
50. Hammad AWA, Akbarnezhad A, Oldfield P. Optimising embodied carbon and U-value in load bearing walls: A mathematical bi-objective mixed integer programming approach. Energy and Buildings. 2018;174:657-71.
51. Xian S, Xu F, Ma C, Wu Y, Xia Q, Wang H, et al. Vapor-enhanced CO_2 adsorption mechanism of composite PEI@ ZIF-8 modified by polyethyleneimine for CO_2/N_2 separation. Chemical Engineering Journal. 2015;280:363-9.